PCCP

Cation Structure-Dependence of the Induced Free Charge Density Gradient in Imidazolium and Pyrrolidinium Ionic Liquids

Journal:	*Physical Chemistry Chemical Physics*
Manuscript ID	CP-ART-03-2022-001066.R1
Article Type:	Paper
Date Submitted by the Author:	14-Jul-2022
Complete List of Authors:	Wang, Yufeng; Michigan State University, Department of Chemistry Adhikari, Laxmi; University of Missouri Baker, Gary; University of Missouri, Chemistry Blanchard, Gary; Michigan State University, Department of Chemistry

Cation Structure-Dependence of the Induced Free Charge Density Gradient in Imidazolium and Pyrrolidinium Ionic Liquids

Yufeng Wang,[1] Laxmi Adhikari,[2] Gary A. Baker[2] and G. J. Blanchard[1,*]
[1] Michigan State University, Department of Chemistry, East Lansing, MI 48824 USA
[2] University of Missouri, Department of Chemistry, Columbia, MO 65211 USA

Abstract

We report on the structure-dependence and magnitude of the induced free charge density gradient (ρ_f) seen in room-temperature ionic liquids (RTILs) with imidazolium and pyrrolidinium cations. We characterize the spatially-resolved rotational diffusion dynamics of a trace-level cationic chromophore to characterize ρ_f in three different pyrrolidinium RTILs and two imidazolium RTILs. Our data show that the magnitude of ρ_f depends primarily on the alkyl chain length of RTIL cation and the persistence length of ρ_f is independent of RTILs cation structure. These findings collectively suggest that mesoscopic structure in RTILs plays a significant role in allowing charge density gradients to form.

* Author to whom correspondence should be addressed: email: blanchard@chemistry.msu.edu, tel: +1 517 353 1105.

Introduction

Room-temperature ionic liquids (RTILs) are salts that exist in the liquid state at room temperature.[1] They typically consist of large organic cations of low symmetry and either organic or inorganic anions.[2] RTILs have a wide range of applications, including their use as substitutes for conventional solvents in some organic syntheses because of their low vapor pressure and high thermal stability.[3-4] RTILs have been used to dissolve biopolymers,[5-6] and as green reaction media for synthesis and catalytic processes.[7-9] RTILs can also be used as lubricants, dispersing agents and antistatic agents.[10-12] RTILs have also found application in supercapacitors, batteries and fuel cells, improving the energy density of these devices.[13-16]

Despite their wide range of applications, there remain questions regarding fundamental issues such as the extent of dissociation, exchange dynamics and the existence of organization in RTILs that extends over length scales well beyond that which are characteristic of liquid solvents.[17-29] Our group has investigated the existence of a free charge density gradient (ρ_f) in RTILs induced by support surface charge.[17, 30-34] We have demonstrated the existence of ρ_f in several 1-alkyl-3-methylimidazolium RTILs, with a characteristic persistence length of *ca*. 70 μm (*vide infra*).[30, 32] The sign of the gradient can by controlled by the polarity of the surface charge of the surface in contact with the RTIL.[31] The magnitude and spatial extent of ρ_f depends on the identity of the RTIL cation and anion as well as the support surface charge density.[32] In ionic solutions the gradient ρ_f is not known to exist over distances beyond the electric double layer. In order for ρ_f to exist in RTILs, individual charged species must be screened sufficiently to prevent efficient recombination due to Coulombic forces and/or charge mobility of discrete ions must be characteristically low. The work we have performed to date has focused on imidazolium-based RTILs and in that work we have evaluated the dependence of ρ_f on the identity of the anion and

on the imidazolium aliphatic chain length. We have not, however, investigated RTILs that use other cations, and that is the purpose of the work we report here.

Another widely used class of RTILs are formed using 1-alkyl-1-methylpyrrolidinium cations. While the pyrrolidinium cation bears passing resemblance to the imidazolium cation (Fig. 1), imidazolium cations possess a substantially delocalized π system. The pyrrolidinium cation, although of the same the ring size, contains no unsaturations and its electronic structure is comparable to other quaternary ammonium cations. This structural difference provides an opportunity to evaluate the role of cation heterocycle electronic structure on the ability of the RTIL to support ρ_f. This is a significant question because the quantity ρ_f is related to the polarizability of the medium,[17, 32-34] and the role of cation headgroup structure in determining the RTIL polarizability is not known. It is known that changing the alkyl chain length of the RTIL cation can alter the degree and nature of ion pairing in RTILs,[35] a factor that influences their physicochemical properties such as density, thermal stability, ionic conductivity, hydrophobicity and viscosity.[36-39] We have found that ρ_f depends on imidazolium cation aliphatic chain length.[32] We expect that the alkyl chain length will also influence ρ_f in pyrrolidinium ionic liquids.

To characterize ρ_f, we measure the fluorescence anisotropy decay of a trace cationic chromophore as a function of distance from an indium doped tin oxide (ITO) support surface to probe ρ_f in the RTIL. We do not vary the surface charge density of ITO, but have chosen this material because it is known to carry an ambient positive surface charge for pH values below six.[40] While the ITO interface is not in an aqueous medium for this work, our previous studies of ρ_f have shown that the sign of the gradient is consistent with ITO carrying a net positive surface charge.[30-31] We characterize ρ_f for three different pyrrolidinium ionic liquids and compare the results to those seen for imidazolium ionic liquids. The pyrrolidinium RTILs we use are 1-butyl-3-

methylpyrrolidinium bis(trifluoromethylsulfonyl)imide ($BMPyrr^+TFSI^-$), 1-hexyl-3-methylpyrrolidinium bis(trifluoromethylsulfonyl)imide ($HMPyrr^+TFSI^-$), and 1-octyl-3-methylpyrrolidinium bis(trifluoromethylsulfonyl)imide ($OMPyrr^+TFSI^-$). The imidazolium RTILs we use are 1-butyl-3-methylimidazolium bis(trifluoromethylsulfonyl)imide ($BMIM^+TFSI^-$) and 1-hexyl-3-methylimidazolium bis(trifluoromethylsulfonyl)imide ($HMIM^+TFSI^-$) (Fig. 1). Understanding how ρ_f depends on RTIL constituent identity will aid in understanding the molecular properties that influence the ability to support a charge density gradient over macroscopic length scales.

Experimental Section

Materials. The pyrrolidinium ionic liquids $BMPyrr^+TFSI^-$, $HMPyrr^+TFSI^-$ and $OMPyrr^+TFSI^-$ were synthesized following methods reported earlier,[41-42] with slight modifications. The preparation of $BMPyrr^+Br^-$ and its subsequent conversion to the $TFSI^-$ salt are described below. The two remaining pyrrolidinium RTILs were prepared by parallel means using the appropriate bromoalkanes.

The synthesis of $BMPyrr^+Br^-$ began by combining 50 mL of ethyl acetate with 15.93 g (0.187 mol) of 1-methylpyrrolidine in a dry 250-mL round-bottom flask. This solution was cooled in an ice water bath and, once cooled, a small molar excess (30.76 g, 1.2 equiv., 0.225 mol) of freshly-distilled 1-bromobutane was added dropwise over the course of 30 min by addition funnel with magnetic stirring under flowing N_2. Following addition of 1-bromobutane, the reaction mixture was removed from the ice bath and stirred overnight at room temperature followed by additional heating at 60 °C for 24 h. After cooling to room temperature, the resulting white to off-white solid product was filtered on a cooled water-jacketed medium sintered glass frit and washed several times with cold ethyl acetate (5 × 20 mL). Residual solvent was removed by rotary

evaporation and, if the product was not pristinely white, the product was further recrystallized from acetonitrile or ethyl acetate and dried under vacuum overnight to obtain a white powder of $BMPyrr^+Br^-$ in 85-90% yield.

To perform anion metathesis, 35.43 g (0.159 mol) of $BMPyrr^+Br^-$ was dissolved in 70 mL water in a 250-mL round-bottom flask. Rapid addition of a solution comprising 50.36 g (1.1 eq., 0.175 mol) of Li^+TFSI^- dissolved in 70 mL of water resulted in almost immediate biphase formation. After vigorous stirring (300-400 rpm) overnight, the stirring was discontinued. After the mixture had been quiescent for at least 1 h, the upper aqueous layer was removed and discarded and the lower RTIL layer was rinsed several times with distilled water (5 × 50 mL) to remove the water-soluble LiBr byproduct. The final product was dried by rotary evaporation for at least 6 h at 60 °C to obtain $BMPyrr^+TFSI^-$ as a colorless liquid (yield: 85-93%). The remaining pyrrolidinium RTILs were prepared similarly. The NMR assignments and integrations are rigorously consistent with the anticipated RTIL structures (see Supporting Information).

$BMIM^+TFSI^-$ (≥98%) and $HMIM^+TFSI^-$ (≥98%) were purchased from Sigma-Aldrich. All RTILs were purified as detailed below before measurement. Activated charcoal (powder, -100 particle size, Sigma-Aldrich) and isopropyl alcohol (99.50%, Macron Fine Chemicals) were used as received. The stock chromophore solution (*ca.* 5×10^{-4} M) of cresyl violet perchlorate (CV^+, Eastman) was prepared by dissolution of the chromophore in ethanol (≥99.5%, Sigma-Aldrich). Water was obtained from a Mili-Q filtration system (Millipore). Indium doped tin oxide (ITO) coated glass slides (10 Ohm/sq, Nanocs) and silicone rubber sheet (MSC Direct) were cleaned as described below prior to use.

RTIL Sample Cell Preparation. The sample cell preparation has been described in detail elsewhere.[30] The closed sample cell confines the RTIL between two glass slides coated by ITO.

ITO-coated slides are cleaned by sonication in detergent (Sparkleen 1, Fisher) solution, Milli-Q water, then isopropyl alcohol for 15 min at each step. The cleaned ITO coated slides are removed from isopropyl alcohol and dried for 30 min at 200 °C. The ITO coated slides are cooled to room temperature in a desiccator and then placed in a UV/ozone cleaner for 20 min. The cell spacer (O-ring, *ca.* 1 mm thick) is cut from a silicone rubber sheet, which is cleaned by sonication in detergent solution and Milli-Q water for 15 min each, then dried by N_2 flow.

Purification of RTILs. The method of RTIL purification has been reported previously.[43] The RTIL is stored over activated carbon for three days. The RTIL is then filtered by syringe filter with a Durapore® poly-(vinylidene difluoride) (PVDF) membrane (0.22 μm sterile filtration, Millex) to separate the RTIL from the activated carbon. The RTIL is then heated for 3 h at 90 °C while stirring and purging with ultrapure Ar (99.9995%, Linde) to minimize water in the RTIL. The water content in purified RTILs is *ca.* 50 ppm, measured by Karl Fischer titration (Mettler-Toledo C10S).

Preparation of CV^+-RTIL Solutions. The CV^+-RTIL solution is prepared by transferring 100 μL of the CV^+ stock solution (*ca.* 5×10^{-4} M) into a vial and placing it in an oven for 3 h at 150 °C to evaporate the solvent ethanol. After removal from the oven and cooling in a desiccator, 1000 μL of purified RTIL is added into the vial to dissolve CV^+. The CV^+-RTIL solution (*ca.* 5×10^{-5} M) is then stirred overnight before use. To minimize water contamination, all glassware is dried for at least 24 h at 150 °C before use.

Characterization of the ρ_f in RTILs. The fluorescence anisotropy decay of the cationic chromophore CV^+ is measured as a function of distance from the ITO support surface to probe the induced free charge density gradient (ρ_f) in the RTILs. A detailed description of the confocal scanning TCSPC imaging system has been reported elsewhere.[30, 44] We control the distance

between the inverted confocal microscope objective and the sample stage mechanically to achieve depth resolution (<1 μm). The time-resolved emission intensity decays are acquired using time-correlated single photon counting (TCSPC) electronics (Becker & Hickl SPC-152) and the laser light source is a cavity dumped synchronously pumped dye laser (Coherent 701-3, Pyrromethene 567 dye, 575 nm, 5 ps pulses, 4 MHz repetition rate, < 1 mW average power at the sample) excited by the second harmonic output (532 nm, 12 ps pulse at 80 MHz repetition rate, 2.5 W average power) of a passively mode-locked Nd:YVO_4 laser (Spectra Physics Vanguard). The instrument response function of this system is < 100 ps.

Results and Discussion

The purpose of this work is to characterize the dependence of ρ_f on the molecular structure of the RTIL cation. We have reported on the dependence of ρ_f on the aliphatic chain length of the imidazolium cation and on the identity of the anion.[32] We characterize ρ_f in three different pyrrolidinium RTILs, and compare those results to ρ_f for imidazolium RTILs. All the RTILs have the same anion ($TFSI^-$) so that complexation data are directly comparable between ionic liquids. We acquire polarized time-resolved emission intensity data using the TCSPC instrument described above. The emission transients polarized parallel ($I_{\|}(t)$) and perpendicular ($I_{\perp}(t)$) to the excitation polarization are used to construct the induced orientational anisotropy decay function, $R(t)$ (Eq. 1).

$$R(t) = \frac{I_{\|}(t) - I_{\perp}(t)}{I_{\|}(t) + 2I_{\perp}(t)} = R(0)\exp\left(-t/\tau_{OR}\right) \qquad [1]$$

For all the data reported here, $R(t)$ decays as a single exponential with a time constant τ_{OR}. The information content of $R(t)$ is well established.[45-52] The zero-time anisotropy, $R(0)$ is a gauge of the angle between the absorbing and emitting transition dipole moments, and the anisotropy decay

time constant, τ_{OR}, is related to system properties through the modified Debye-Stokes-Einstein equation (Eq. 2).[46]

$$\tau_{OR} = 6D^{-1} = \frac{\eta V f}{k_B T S} \quad [2]$$

In Eq. 2, η is the viscosity of the medium in which the chromophore is reorienting, V is the hydrodynamic volume of the rotating entity,[47] f is the frictional boundary condition term[49] and S is a factor to account for the ellipsoidal shape of the rotating entity.[51] We have established that the free charge density gradient, ρ_f, is related to the spatial variation in τ_{OR} through the volume of the reorienting entity,[30] which is the weighted average of the free and complexed chromophore (Eqs. 3 and 4),

$$\nabla \cdot \tau_{OR} = \left(\frac{\eta f}{k_B T S} \right) \nabla \cdot V = k \nabla \cdot V \quad [3]$$

$$\nabla \cdot V = V_{free} \nabla \cdot X_{free} + V_{complex} \nabla \cdot X_{complex} \quad [4]$$

In RTILs, charged chromophores form complexes with the dissociated RTIL constituents of opposite charge.[30, 32] The position-dependent change in the measured reorientation time constant ($\nabla \cdot \tau_{OR}$) is a consequence of a concentration gradient of RTIL charged species that results from the presence of the surface charge on the support. This gradient is manifested as a gradient in hydrodynamic volume of the rotating entity ($\nabla \cdot V$). Thus, $\nabla \cdot \tau_{OR}$ reflects the induced free charge density gradient in RTILs (Scheme 1).

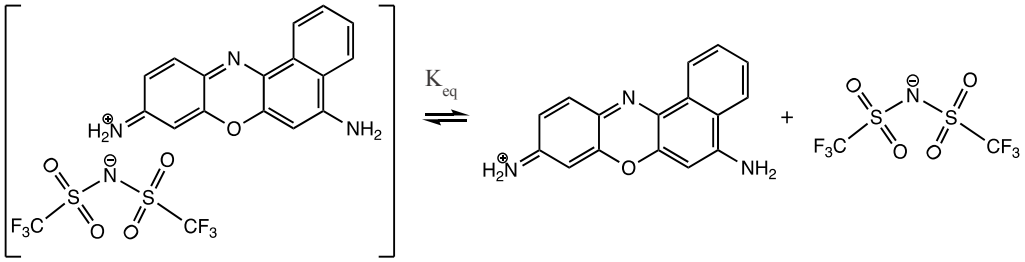

Scheme 1: Equilibrium between CV^+ and RTIL anion $TFSI^-$.

Because the RTILs used here have a common anion, $TFSI^-$, the same chromophore-RTIL anion complex is formed in all the RTILs examined. The identity of the RTIL constituents determine the viscosity of the medium and K_{eq} (Scheme 1), as well as the extent of RTIL dissociation.[35] For RTILs, the nature of chromophore solvation is much more complicated and challenging to model at the molecular level than it would be in dilute solution, as Scheme 1 may seem to imply. The numerous exchange processes that operate in RTILs collectively determine the observed bulk properties,[35] and the CV^+ chromophore participates in these processes. There is a characteristic free energy of interaction for the CV^+-$TFSI^-$ ion pair and the equilibrium constant indicated in Scheme 1 will certainly be very different from a dilute solution limit equilibrium constant for the same ions. The only assumptions we make in our treatment of the data are that ionic association and dissociation do occur, the process is characterized by a free energy, and that LeChatelier's principle applies. The concentration of dissociated $TFSI^-$ will determine the relative amounts of free CV^+ and complexed CV-TFSI are present. The magnitude of ρ_f can be evaluated by measuring the variation of [$TFSI^-$] with distance from the charged support. The depth-dependent τ_{OR} data for CV in $BMPyrr^+TFSI^-$, $BMIM^+TFSI^-$, $HMPyrr^+TFSI^-$, $HMIM^+TFSI$ and $OMPyrr^+TFSI^-$ are presented in Fig. 2. The observed ρ_f does depend on the aliphatic chain length of both the pyrrolidinium and imidazolium cations. The measured reorientation time constants in

the ionic liquids are consistent with the predictions of Eq. 2 based on the reported RTIL bulk viscosities.[38, 53-55]

While the structural details of RTILs that allow them to support the establishment of ρ_f remain under investigation, it is useful to consider the possible means by which ρ_f forms. As shown in Table 1, the magnitude of ρ_f is on the order of ca. 20 μC/cm^3/μm. To place this value in perspective, if the RTIL is 50% dissociated,[35] the steady state concentration of ionized species is *ca*. 2 M, depending on the specific RTIL. The steady state charge density for a 2 M solution is *ca*. 200 C/cm^3. The gradient we report is thus *ca*. 0.1 ppm/μm of the charge density present in the system.[32] Regardless, the establishment of such a gradient requires the displacement of charge and RTILs are characterized by relatively high viscosities (Table 1). Our measurements require tens of minutes to acquire a full dataset, and during that timeframe there is no observed change in or evolution of ρ_f. Likewise, there is no waiting time required for ρ_f to develop prior to measurement. For this reason, it is likely the establishment of ρ_f is mediated by the kinetics of RTIL association and dissociation rather than by ion translational motion, and this is a matter under investigation. We note that ρ_f is seen to persist in RTILs upon dilution with molecular solvents up to ca. 30 mole% diluent. Even at higher dilutions, persistent aggregation of RTILs is seen, suggesting the importance of RTIL local organization in establishing and mediating ρ_f.[34]

The data shown in Fig. 2 demonstrate the presence of ρ_f, but direct comparison of the magnitude and persistence length of ρ_f is more facile when the data are normalized. We use the quantity $\Delta\tau_{OR}/\tau_{OR} = ((\tau_{OR}^0-\tau_{OR}^\infty)/\tau_{OR}^\infty)$ to facilitate the comparison, where the denominator term is taken to be τ_{OR} in the bulk RTIL, where ρ_f has decayed fully. As shown in Fig. 3a, $\Delta\tau_{OR}/\tau_{OR}$ is larger in the pyrrolidinium RTILs with longer alkyl chain (OMPyrr$^+$TFSI$^-$ > HMPyrr$^+$TFSI$^-$ ≥ BMPyrr$^+$TFSI$^-$). The analogous dependence is also seen in imidazolium ionic liquids (Fig. 3b).

Comparison of the pyrrolidinium and imidazolium RTILs with same cation aliphatic chain length (Fig. 4) shows that $\Delta\tau_{OR}/\tau_{OR}$ is indistinguishable in magnitude and persistence length for $BMPyrr^{+}TFSI^{-}$ and $BMIM^{+}TFSI$ (Fig. 4a) but there appears to be a slight difference in the slope of the decay of $\Delta\tau_{OR}/\tau_{OR}$ for $HMPyrr^{+}TFSI^{-}$ and $HMIM^{+}TFSI^{-}$ (Fig. 4b). We note that for all data points in Fig. 4b, the values of $\Delta\tau_{OR}/\tau_{OR}$ for a given distance, *d*, are the same to within the experimental uncertainty.

From the data presented in Figs. 4 we can determine the magnitude of ρ_f.[32] To characterize the gradient, we need to establish the difference in amount of CV^{+} that is complexed at $d = 0$ and the amount complexed at distances *d* where the $\rho_f = 0$ (designated $x=\infty$ in Eq. 5). Measuring such quantities directly is not feasible, but they can be estimated by the change in hydrodynamic volume of the reorienting entity. The calculation of hydrodynamic volume has been demonstrated to be reliable, and from the volume change data (Eq. 5) and an estimate of K_{eq} for the CV^{+}-$TFSI^{-}$ complex, we can relate the concentration gradient in the RTIL anion over the decay of the normalized reorientation time gradient (Eq. 6), which is proportional to ρ_f. V_{RI} is the hydrodynamic volume of the RTIL ion which forms a complex with the chromophore. In this work, $V_{RI} = V_{(TFSI^{-})} = 169$ Å^3.[47]

$$\frac{\Delta\tau_{OR}}{\tau_{OR}} = \frac{\Delta V}{V} = \frac{(X_{free}^{x=0\,\mu m} - X_{free}^{x=\infty})\cdot V_{RI}}{V_{complex} - X_{free}^{x=\infty}\cdot V_{RI}} \qquad [5]$$

$$\frac{\Delta\tau_{OR}}{\tau_{OR}}(x) = \frac{\Delta\tau_{OR}}{\tau_{OR}}(0)\exp(-x/d) \qquad [6]$$

The functional form of Eq. 6 has been established empirically in our lab.[17, 30-33] The quantity $(\Delta\tau_{OR}/\tau_{OR})(x)$ reflects the concentration gradient in the RTIL anion, and we relate these data to ρ_f

as described previously (Table 1).[32] Several important points emerge from these data. The first point is that ρ_f depends on the RTIL cation aliphatic chain length, but not on the identity of the cationic headgroups (pyrrolidinium and imidazolium). In all cases the gradient is modest. The values of ρ_f do not match precisely those that were reported previously[32] and this is not surprising. The magnitude of the gradient necessarily depends on the surface charge density of the support,[31] a quantity that can vary from lot-to-lot for the ITO deposited on the support surface. The results reported here, however, are all acquired using the same lot of ITO-coated glass and are thus comparable. The significance of these results is that ρ_f appears to be comparatively insensitive to the identity of the cation headgroup for the two species reported here, but ρ_f is seen to depend more sensitively on cation aliphatic chain length. This finding appears somewhat surprising given that the presence of unsaturation in the imidazolium headgroup would suggest greater polarizability than would be seen in the pyrrolidinium headgroup. Given that aliphatic chains are characterized by modest dielectric constants, it appears that the molecular-scale organization for these systems, which is known to exist,[56-60] can influence the ability to support a free charge density gradient. For such systems, the notion of polarizability may not be strictly associated with the molecular entities present in the system. Rather, the dielectric response of the RTIL, which will depend on the details of local organization in the medium, is likely dominated by (transient) structures comprised of more than individual contact ion pairs and free ions. X-ray diffraction data have revealed mesoscopic organization consistent with this possibility[57-61] and extent to which aggregate structures are responsible for this organization would likely depend more sensitively on the RTIL cation aliphatic chain length than cationic headgroup identity. Our observation that RTILs can support a charge density gradient across macroscopic distances argues for the importance of mesoscopic organization in determining system properties.

We also evaluate the spatial extent of ρ_f. The spatial dependence of ρ_f is given by Eq. 6,[33] where d is the e^{-1} characteristic persistence length of ρ_f. By fitting the experimental ρ_f to this function, we can obtain the value of d. The data in Table 1 also show that the persistence length of ρ_f is the same to within the experimental uncertainty for all the RTIL structures reported here. The apparent structural independence of d suggests a physical rather than a chemical basis for determining ρ_f, and this finding is consistent with the existence of mesoscopic organization in RTILs. For dipolar systems the presence of an E field can serve to orient the dipoles and the interaction between the E field and the dipolar constituents is described in terms of induced polarization. For systems that are not strictly dielectric media, but possess some nominally free carrier density, the spatial extent of the induced polarization will be attenuated. For RTIL systems characterized by similar extents of dissociation,[35] as is the case for the pyrrolidinium and imidazolium RTILs, one would expect the distance over which the induced polarization would persist to be similar.

Conclusions

We have examined the cation structure-dependence of the induced free charge density gradient (ρ_f) for pyrrolidinium and imidazolium RTILs. We find that the magnitude of ρ_f depends primarily on the cation aliphatic chain length and differs little with the identity of the charge-carrying cation headgroup. An implication of these findings is that local organization in the RTILs that is mediated by the nonpolar constituent of the cation plays a significant role in the ability of these systems to support a charge density gradient over macroscopic distances. Conversely, we find that the characteristic persistence length of ρ_f is the same for all RTILs examined here. This finding could be accounted for by the extent of RTIL dissociation, which is similar for the RTILs

studied here. Taken collectively, these data provide additional insight into the physical and structural factors that are most important in determining ρ_f in RTILs.

Supporting Information

^{1}H NMR spectra of RTILs and derivation of Eq. 5.

Acknowledgement

This research was carried out under the framework of project #W911-NF-14-10063 funded by the Army Research Office.

Table 1. Magnitude and Persistence Length of ρ_f in Imidazolium and Pyrrolidinium RTILs.

RTIL	η (cP)	$\Delta\tau_{OR}/\tau_{OR}$	ΔC (mol/L)	ρ_f ((μC/cm^3)/μm)	d (μm)
OMPyrr$^+$TFSI$^-$	130[38]	0.24±0.02	(2.34±0.19)×10^{-5}	23±2	76±3
HMPyrr$^+$TFSI$^-$	98[55]	0.17±0.02	(1.58±0.34)×10^{-5}	15±3	75±1
HMIM$^+$TFSI$^-$	81[53]	0.20±0.02	(1.82±0.28) ×10^{-5}	18±3	66±6
BMPyrr$^+$TFSI$^-$	78[38]	0.14±0.02	(1.2±0.16) ×10^{-5}	12±1	74±3
BMIM$^+$TFSI$^-$	52[54]	0.13±0.01	(1.3±0.16) ×10^{-5}	13±1	69±5

References

1. P. M. Dean; J. M. Pringle; D. R. MacFarlane, *Chem. Phys. Phys. Chem.* **2010,** *12*, 9144-1953.

2. M. D. Joshi; J. L. Anderson, *RSC Advances* **2012,** *2*, 5470-5484.

3. G. Durga; A. Mishra, *Ionic Liquids: Industrial Applications*. Wiley: 2016.

4. R. D. Rogers; K. R. Seddon, *Science* **2003,** *302*, 792-793.

5. H. Garcia; R. Ferriera; M. Petkovic; J. L. Ferguson; M. C. Leitao; H. N. Gunaratne; K. R. Seddon; L. P. N. Rebelo; C. S. Periera, *Green Chem.* **2010,** *12*, 367-369.

6. K. Wilpiszewska; T. Spychaj, *Carbohydr. Polym.* **2011,** *86*, 424-428.

7. J. P. Hallett; T. Welton, *Chem. Rev.* **2011,** *111*, 3508-3576.

8. R. L. Vekariya, *J. Mol. Liq.* **2017,** *227*, 44-60.

9. J. S. Yadav; B. V. S. Reddy; K. Premalatha, *Adv. Synth. Catal.* **2003,** *345*, 948-952.

10. C. J. Reeves; A. Siddaiah; P. L. Menezes, *J. Clean. Prod.* **2018,** *176*, 241-250.

11. B. Weyershausen; K. Lehmann, *Green Chem.* **2005,** *7*, 15-19.

12. H. Zhao, *Chem. Eng. Commun.* **2006,** *193*, 1660-1677.

13. M. Armand; F. Endres; D. R. MacFarlane; H. Ohno; B. Scrosati, *Ionic Liquid Materials for the Electrochemical Challenges of the Future*. World Scientific: 2010.

14. D. R. MacFarlane; N. Tachikawa; M. Forsyth; J. M. Pringle; P. C. Howlett; G. D. Elliott; J. H. Davis; M. Watanabe; P. Simon; C. A. Angell, *Energ. Env. Sci.* **2014,** *7*, 232-250.

15. B. Qiu; B. Lin; F. Yan, *Polym. Int.* **2013,** *62*, 335-337.

16. K. L. van Aken; M. Beidaghi; Y. Gogotsi, *Angew. Chem. Int. Ed. Engl.* **2015,** *127*, 4888-4891.

17. Y. Wang; F. Parvis; M. I. Hossain; K. Ma; R. Jarosova; G. M. Swain; G. J. Blanchard, *Langmuir* **2021,** *37*, 605-615.

18. R. S. Anaredy; S. K. Shaw, *Langmuir* **2016,** *32*, 5147-5154.

19. R. S. Anaredy; S. K. Shaw, *J. Phys. Chem. C* **2018,** *122*, 19731-19737.

20. R. S. Anaredy; S. K. Shaw, *J. Phys. Chem. C* **2019,** *123*, 8975-8982.

21. S. Baldelli, *J. Phys. Chem. Lett.* **2013,** *4*, 244-252.

22. M. A. Gebbie; H. A. Dobbs; M. Valtiner; J. N. Israelachvilli, *Proc. Nat. Acad. Sci. USA* **2015,** *112(24)*, 7432-7437.

23. M. A. Gebbie; M. Valtiner; X. Banquy; E. T. Fox; W. A. Henderson; J. N. Israelachvilli, *Proc. Nat. Acad. Sci. USA* **2013,** *110(24)*, 9674-9679.

24. J. Nishida; J. P. Breen; B. Wu; M. D. Fayer, *ACS Cent. Sci.* **2018,** *4*, 1065-1073.

25. J. Y. Shin; S. A. Yamada; M. D. Fayer, *J. Am. Chem. Soc.* **2017,** *139*, 311-323.

26. J. Y. Shin; S. A. Yamada; M. D. Fayer, *J. Am. Chem. Soc.* **2017,** *139*, 11222-11232.

27. J. E. Thomaz; H. E. Bailey; M. D. Fayer, *J. Chem. Phys.* **2017,** *147*, 194502 1-11.

28. B. Wu; J. P. Breen; M. D. Fayer, *J. Phys. Chem. C* **2020,** *124*, 4179-4189.

29. B. Wu; J. P. Breen; X. Xing; M. D. Fayer, *J. Am. Chem. Soc.* **2020,** *142*, 9482-9492.

30. K. Ma; R. Jarosova; G. M. Swain; G. J. Blanchard, *Langmuir* **2016,** *32*, 9507-9512.

31. K. Ma; R. Jarosova; G. M. Swain; G. J. Blanchard, *J. Phys. Chem. C* **2018,** *122*, 7361-7367.

32. Y. Wang; R. Jarosova; G. M. Swain; G. J. Blanchard, *Langmuir* **2020,** *36*, 3038-3045.

33. Y. Wang; G. M. Swain; G. J. Blanchard, *J. Phys. Chem. B* **2021,** *125*, 950-955.

34. M. I. Hossain; G. J. Blanchard, *Phys. Chem. Chem. Phys.* **2022,** *24*, 3844-3853.

35. O. Nordness; J. F. Brennecke, *Chem. Rev.* **2020,** *120*, 12873-12902.

36. K. R. Harris; L. A. Woolf; M. Kanakubo; T. Ruther, *J. Chem. Eng. Data* **2011,** *56*, 4672-4685.

37. J. G. Huddleston; A. E. Visser; W. M. Reichert; H. D. Willauer; G. A. Broker; R. D. Rogers, *Green Chem.* **2001,** *3*, 156-164.

38. J. Salminen; N. Papaiconomou; R. A. Kumar; J. M. Lee; J. Kerr; J. Newman; J. M. Prausnitz, *Fluid Phase Equil.* **2007,** *261*, 421-426.

39. H. Tokuda; K. Ishii; M. A. B. H. Susan; S. Tsuzuki; K. Hayamizu; M. Watanabe, *J. Phys. Chem. B* **2006,** *110*, 2833-2839.

40. T. A. N. Peiris; S. Senthilarasu; K. G. U. Wijayantha, *J. Phys. Chem. C* **2012,** *116*, 1211-1218.

41. A. K. Burrell; R. E. Del Sesto; S. N. Baker; T. M. McCleskey; G. A. Baker, *Green Chem.* **2007,** *9*, 449-454.

42. G. A. Baker; S. Pandey; S. Pandey; S. N. Baker, *Analyst* **2004,** *129*, 890-892.

43. R. Jarosova; G. M. Swain, *J. Electrochem. Soc.* **2015,** *162*, H507-H511.

44. C. E. Hay; F. Marken; G. J. Blanchard, *Langmuir* **2014,** *30*, 9951-9961.

45. T. J. Chuang; K. B. Eisenthal, *J. Chem. Phys.* **1972,** *57*, 5094-5097.

46. P. M. Debye, *Polar Molecules*. Chemical Catalog Co.: New York, 1929.

47. J. T. Edward, *J. Chem. Ed.* **1970,** *47*, 261-270.

48. L. D. Favro, *Phys.. Rev.* **1960,** *119*, 53-62.

49. C.-M. Hu; R. Zwanzig, *J. Chem. Phys.* **1974,** *60*, 4354-4357.

50. J. R. Lakowicz, *Fluorescence Anisotropy*. Springer: Boston, MA, 1999.

51. F. Perrin, *J. Phys. Radium* **1934,** *5*, 497.

52. T. Tao, *Biopolymers* **1969,** *8*, 609-632.

53. J. C. F. Diogo; F. J. P. Caetano; J. M. N. A. Fareleira; W. A. Wakeham, *Int. J. Thermophys.* **2014,** *35*, 1615-1635.

54. K. R. Harris; M. Kanakubo, *Phys. Chem. Chem. Phys.* **2015,** *17*, 23977-23993.

55. A. R. C. Morais; L. M. Alaras; D. L. Baek; R. V. Fox; M. B. Shiflett; A. M. Sucurto, *J. Chem. Eng. Data* **2019,** *64*, 4658-4667.

56. J. Schaffer; M. Alber; W. Korth; M. Cokoja; A. Jess, *Chem. Eur.* **2017,** *2*, 11891-11898.

57. A. Triolo; O. Russina; H.-J. Blief; E. Di Cola, *J. Phys. Chem. B* **2007,** *111*, 4641-4644.

58. J. Dupont, *J. Braz. Chem. Soc.* **2004,** *15*, 341-350.

59. C. S. Santos; N. S. Murthy; G. A. Baker; E. W. Castner Jr., *J. Chem. Phys.* **2011,** *134*, 121101 (1-4).

60. H. V. R. Annapureddy; H. K. Kashyap; P. M. De Biase; C. J. Margulis, *J. Phys. Chem. B* **2010,** *114*, 16838-16846.

61. O. Russina; A. Triolo; L. Gontrani; R. Caminiti, *J. Phys. Chem. Lett.* **2012,** *3*, 27-33.

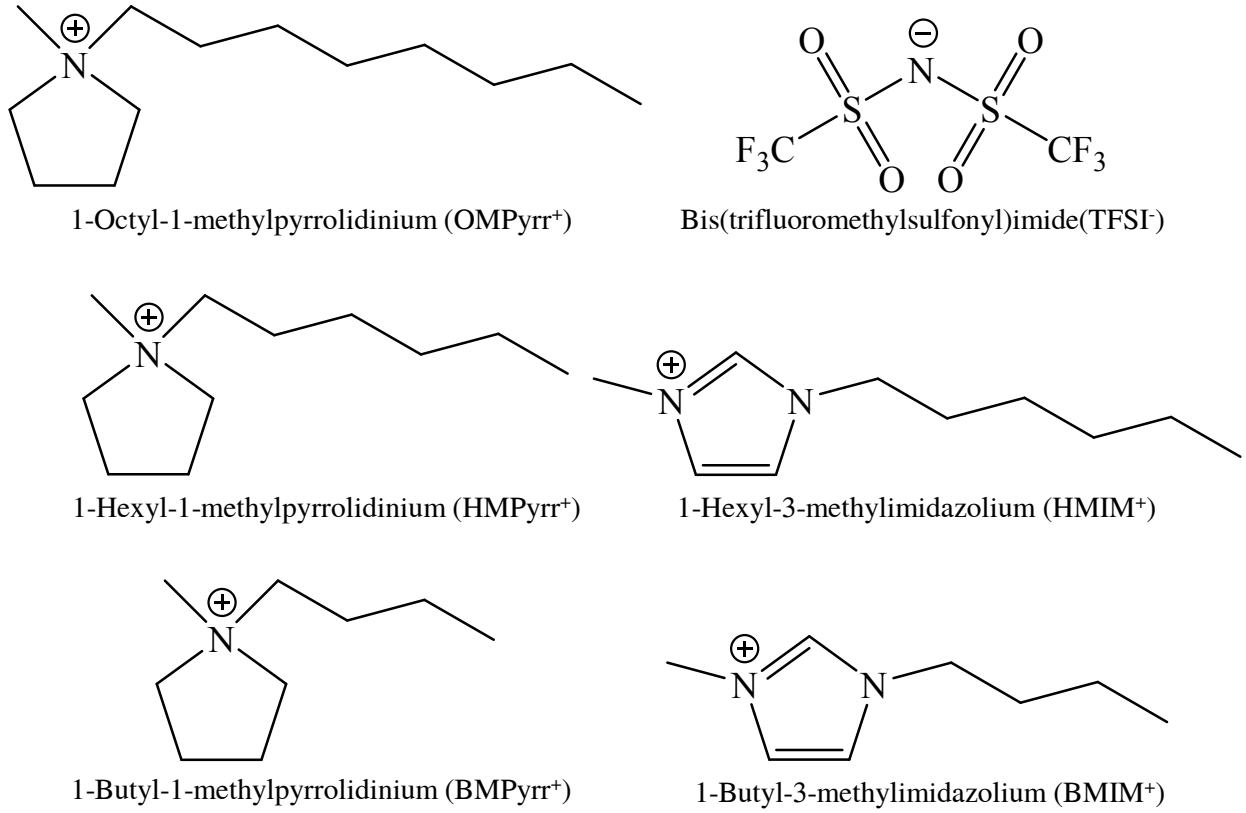

Figure 1. Structures of the RTIL constituents used in this work.

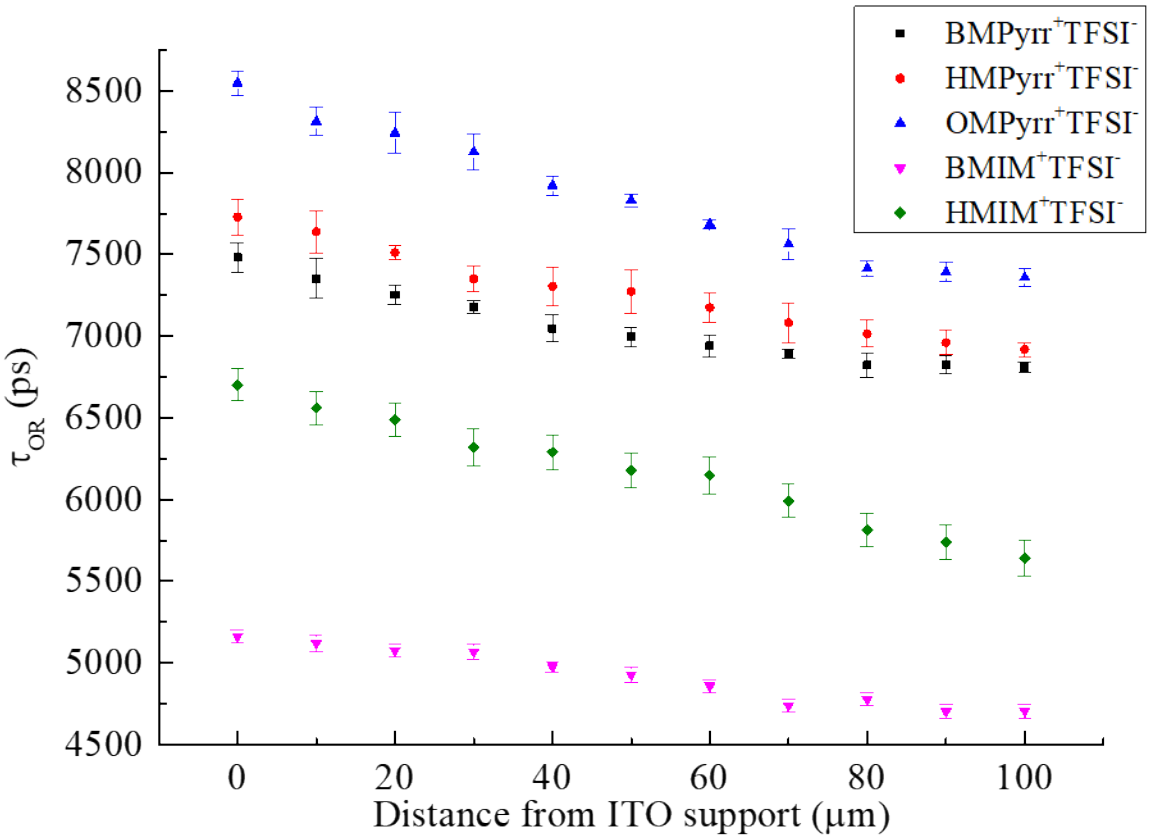

Figure 2. Cresyl violet anisotropy decay time constants as a function of RTIL cation alkyl chain length, with the same anion. Black squares represent for $BMPyrr^{+}TFSI^{-}$, red circles are $HMPyrr^{+}TFSI^{-}$, blue triangles are $OMPyrr^{+}TFSI^{-}$, purple inverted triangles are $BMIM^{+}TFSI^{-}$, and green diamonds are $HMIM^{+}TFSI^{-}$. For all data points, n=3.

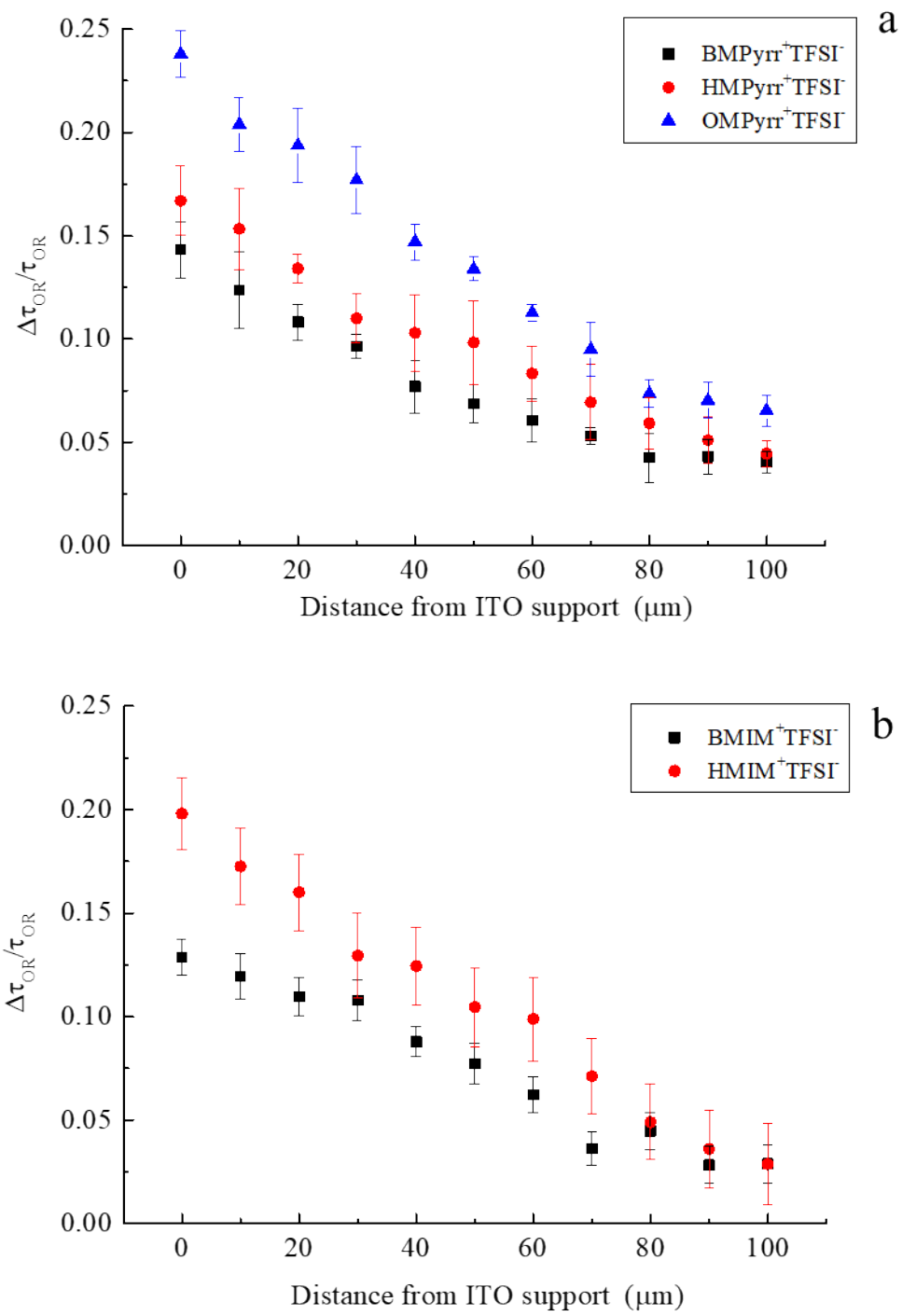

Figure 3. Normalized anisotropy decay time gradient ($\Delta\tau_{OR}/\tau_{OR}$) of Cresyl violet, as a function of distance from ITO support and RTIL cation alkyl chain length (a) Black squares represent for $BMPyrr^{+}TFSI^{-}$, red circles are $HMPyrr^{+}TFSI^{-}$ and blue triangles are $OMPyrr^{+}TFSI^{-}$. (b) Black squares are $BMIM^{+}TFSI^{-}$ and red circles are $HMIM^{+}TFSI^{-}$. For all data points, n=3.

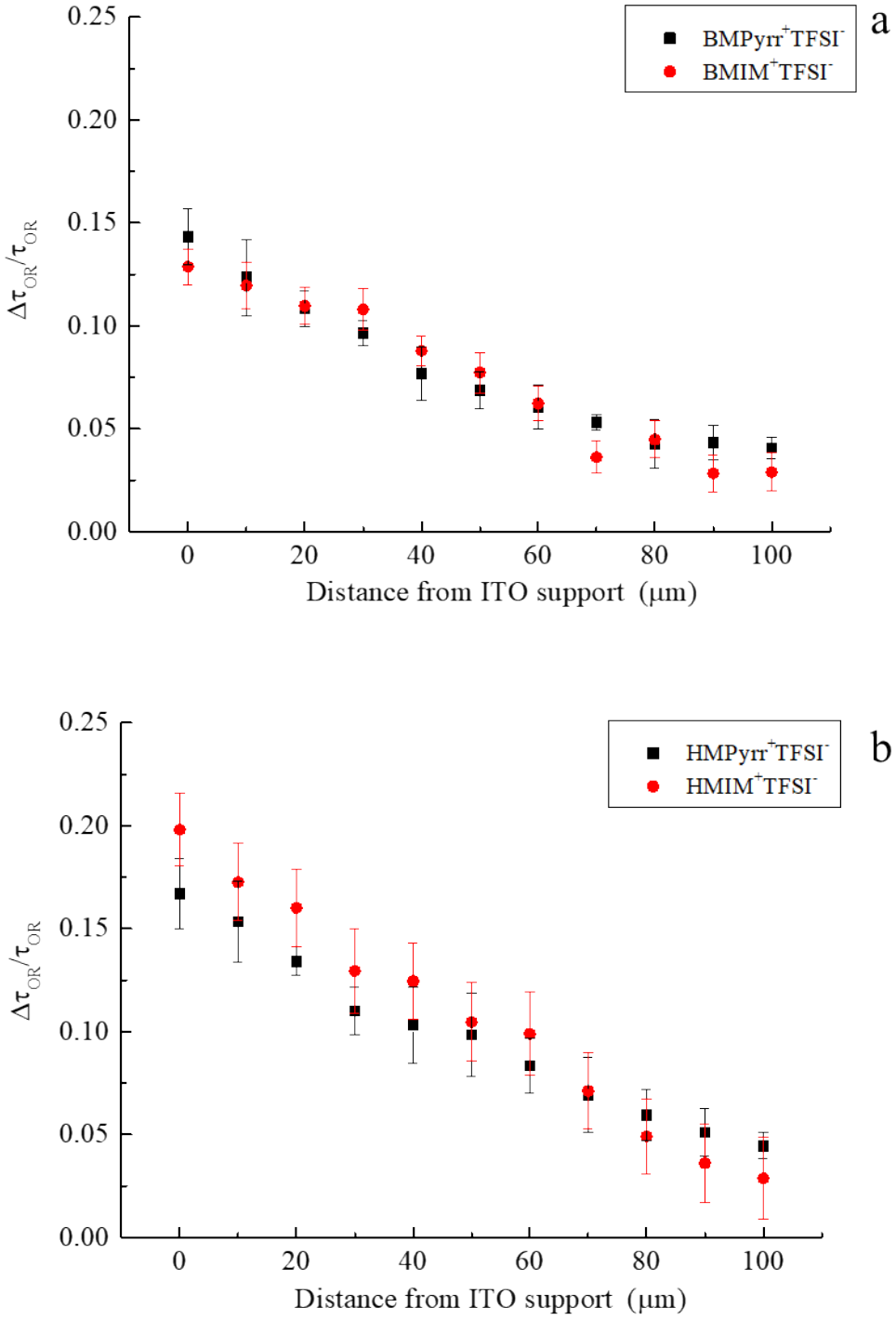

Figure 4. Comparison of the normalized anisotropy decay time gradient ($\Delta\tau_{OR}/\tau_{OR}$) of Cresyl violet in pyrrolidinium and imidazolium RTILs with same cation alkyl chain length (a) Black squares represent for $BMPyrr^{+}TFSI^{-}$ and red circles are $BMIM^{+}TFSI^{-}$. (b) Black squares are $HMPyrr^{+}TFSI^{-}$ and red circles are $HMIM^{+}TFSI^{-}$. For all data points, n=3.